

Decimated Photonic Crystal Defect Cavity Lasers

Antonios V. Giannopoulos, *Student Member, IEEE*, Joshua D. Sulkin, *Student Member, IEEE*, Christopher M. Long, *Student Member, IEEE*, James J. Coleman, *Fellow, IEEE*, and Kent D. Choquette, *Fellow, IEEE*

Abstract—We present the design, fabrication, and characterization of decimated lattice photonic crystal membrane lasers. Based on our simulated designs, decimated photonic crystal lattices have reduced number of holes, which enhance the current and heat conductive paths from the optical cavity with a minimal impact on the cavity quality factor and resonance. Our calculations indicate lower operating temperature using the decimation lattice designs. Two decimated cavity designs are demonstrated and compared to conventional photonic crystal defect cavity lasers in InP-based membranes. The decimated designs show improved laser performance with a small reduction of measured cavity quality factor. Reduction of the photonic crystal holes around the defect cavity to as few as two periods still enables photopumped operation of photonic crystal defect lasers. The improvement in the thermal properties is characterized by varying the photopumping duty cycle.

Index Terms—Photonic bandgap materials, semiconductor lasers.

I. INTRODUCTION

PROGRESS in semiconductor fabrication technologies has allowed researchers to exploit the characteristics of photonic crystals at optical wavelengths. Recently 2-D photonic crystal membranes have been utilized to create nanoscale lasers [1]. Since their discovery, much study has been pursued to increase the cavity quality factor [2]–[4] and decrease the modal volume [5] of these lasers. There still remains much study to be done in the optimization of the thermal and electrical conductivities of photonic crystal membrane lasers, which is critical for diode operation [6], [7]. Since most membrane lasers are suspended in air and perforated with holes, the thermal and electrical conductivities are degraded. This has contributed to only a few examples of electrically injected photonic crystal membrane emitters [8]–[10]. Wafer bonding techniques have been pursued to provide better heat sinking, which generally improves the laser performance and can lead to room-temperature continuous-wave lasing [11]–[13]. However, since the substrates onto which the photonic crystal membranes are transferred are

often low index, nonconductive dielectrics, the electrical properties of the devices are for the most part unaltered.

Previous photonic crystal cavities have omitted or modified the holes in the lattice to obtain single-mode operation [14]. The modal symmetry was exploited to selectively increase the loss of certain modes. In our paper, the omission of holes in a photonic crystal cavity is motivated by the subsequent increase in semiconductor material to increase the electrical and thermal conductivities. Our decimated photonic crystal cavities exhibit quality factors close to those of complete photonic crystal cavities, but can have a significantly fewer number of air holes. Since the omitted holes form a semiconductor path toward the optical cavity, the thermal impedance and electrical resistance from the center of the cavity to the bulk membrane will both decrease. We first describe a design approach for elimination of holes in a periodic lattice as well as thermal simulations. We then describe the fabrication and characterization of two decimated photonic crystal designs, which exhibit improved laser performance.

II. DECIMATION SIMULATION

The decimation design approach is relatively straightforward. Air holes are omitted from locations in which there is little overlap with the mode and are thus not necessary. We consider two photonic crystal designs that have produced high quality factor cavities: L3 and H2 defect cavity lasers. The L3 cavity is formed in a hexagonal photonic crystal by omitting three holes along the Γ -K direction [4]. The H2 defect cavity has seven holes omitted in a hexagonal lattice, where the innermost hole diameter and position are altered to increase the cavity quality factor [15].

A simple algorithm is used as a guide to help determine which air holes can be removed. First, a 2-D finite-difference time-domain (FDTD) simulation is used to calculate the modal profile. Circular sectors are then drawn from the outside of the cavity to the edge of the simulation domain, and the field intensities within each sector are summed. Fig. 1 shows the sectors, with the color representing the sum of the field intensities, for calculated modes in the two cavities. Holes are removed if they overlap completely with sectors that are in the bottom p percentile of summed intensities (however, holes in the inner two rows are never removed). The number of holes removed is controlled by the value of p , which in Fig. 1 is chosen to be 20% and 65% for the L3 and H2 cavities, respectively. In the final, fabricated design, additional holes are removed by manual inspection.

To study the effects of lattice decimation, we have also performed 3-D FDTD method calculations of the resonant wavelengths, quality factors, and modal profiles for the L3 and decimated L3 cavities. For the lasers fabricated in this paper,

Manuscript received December 1, 2010; revised February 18, 2011; accepted April 4, 2011. Date of publication May 27, 2011; date of current version December 7, 2011. This work was supported by the National Science Foundation under Award ECCS 07-25515.

A. V. Giannopoulos is with MicroLink Devices, Niles, IL 60714 USA.

J. D. Sulkin, J. J. Coleman, and K. D. Choquette are with the Department of Electrical and Computer Engineering, University of Illinois at Urbana-Champaign, Urbana, IL 61801 USA (e-mail: sulkin@illinois.edu; jcoleman@illinois.edu; choquett@illinois.edu).

C. M. Long is with the School of Electrical and Computer Engineering, Purdue University, West Lafayette, IN 47907 USA.

Color versions of one or more of the figures in this paper are available online at <http://ieeexplore.ieee.org>.

Digital Object Identifier 10.1109/JSTQE.2011.2141975

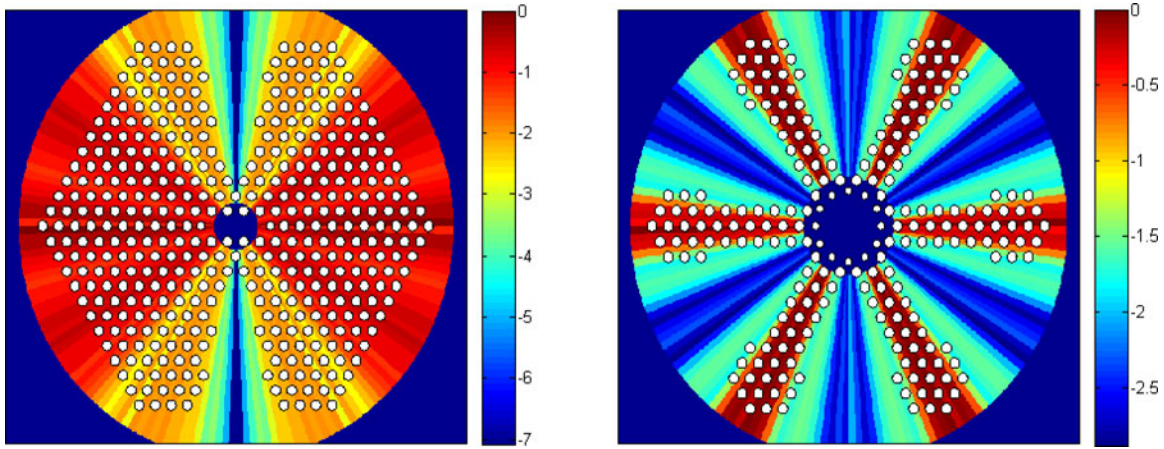


Fig. 1. Depiction of the algorithm used to help determine which holes are removed in a decimated design for (a) L3 ($a = 370$ nm) and (b) H2 ($a = 450$ nm) cavities. The summed field intensities in each sector are on a log scale.

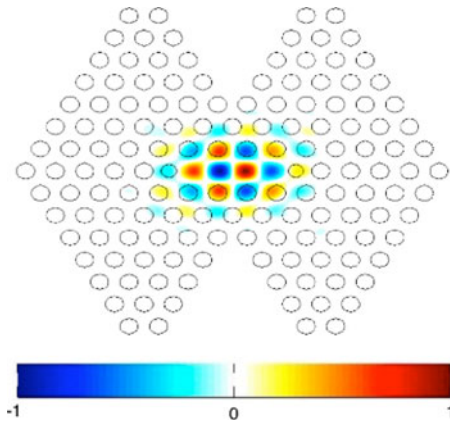


Fig. 2. Modal profile (magnetic field component) of decimated L3 photonic crystal defect cavity ($a = 470$ nm) determined by 3-D FDTD calculation.

the membrane is 135 nm thick, the nearest neighbor hole spacing a is 470 nm, and the hole radius is $0.3a$. The two holes at the ends of the cavity are made slightly smaller ($0.25a$) than the other holes and shifted away from the center of the cavity by $0.15a$. In the simulation, the refractive index of the membrane is assumed to be 3.4. For the L3 cavity, the calculated mode predominantly occupies regions on the right and left of the waveguide cavity. This allows for the removal of holes above and below the cavity without significantly affecting the optical confinement, in agreement with our 2-D simulations. The cavity is decimated by the removal of ten holes above and below the cavity, and the resonance, modal profile, and quality factor are calculated again. The modal profile is shown in Fig. 2. There is no significant change in the resonant wavelength and to the modal distribution after the decimation process. The calculated quality factor for the decimated cavity is approximately 17% less than that of the full cavity.

In order to qualitatively evaluate the thermal behavior of the decimated cavities, a time-independent heat transfer analysis using a finite-element method is performed. The photonic crystal membrane laser is simplified to be a body of revolution, and the thermal conductivity to be a volumetric average that is pro-

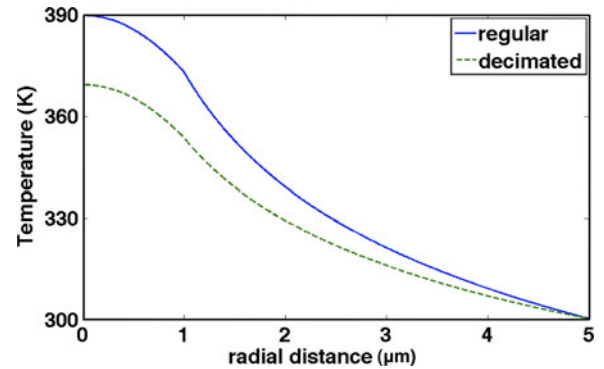


Fig. 3. Calculated temperature profile as a function of the distance from the center of the cavity of an H2 (solid) and a decimated H2 cavity design (dashed).

portional to the effective fill factor of the photonic crystal. The thermal conductivity of the bulk membrane (without holes) is assumed to be 4.2 W/m-K [16]. The source is assumed to have a spot size of $2 \mu\text{m}$, a wavelength of 980 nm, and an incident power of 0.3 mW. The heat sink temperature is taken to be 300 K. Fig. 3 shows the calculated temperature profiles for the H2 cavity laser and a decimated H2 laser [as depicted in Fig. 1(b)]. The semiconductor fill factor for the conventional H2 cavity is 63%, while the fill factor for the decimated H2 cavity increases to 83%. As shown by the comparison of the temperature profiles of the two cavities in Fig. 3, the increase in fill factor for the decimated H2 cavity results in a calculated 20 K temperature decrease at the cavity. It is likely that the actual thermal conductivity improvements are greater since the decimated cavity has large regions of connected semiconductor material surrounding the cavity.

III. FABRICATION

Decimated and full L3 photonic crystal defect cavities are fabricated in a 135-nm-thick InGaAsP membrane grown on an InP substrate. The membrane contains five quantum wells with a nominal photoluminescence peak at 1350 nm. A SiO_2 layer is deposited on the sample, patterned using electron beam

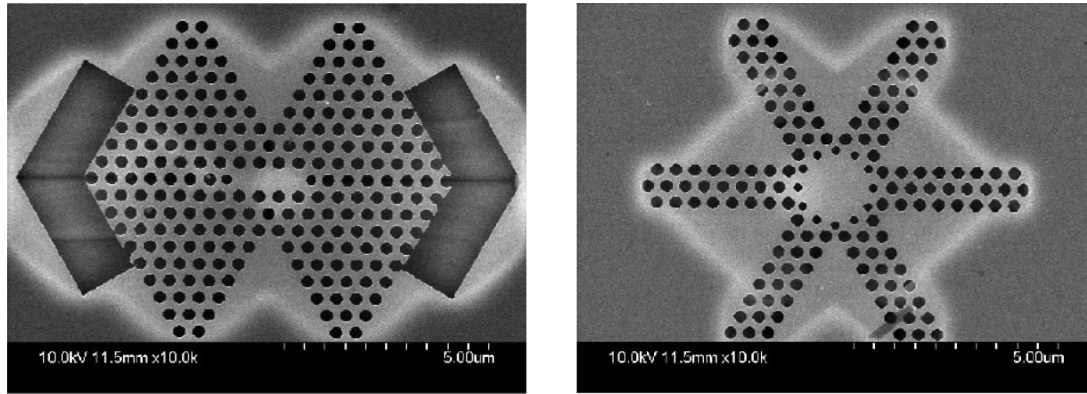


Fig. 4. (a) Fabricated decimated L3 and (b) H2 photonic crystal defect cavity lasers.

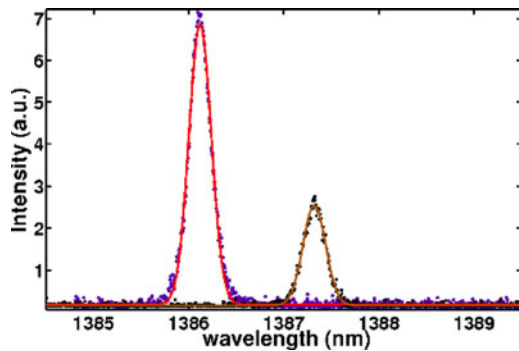


Fig. 5. Subthreshold spectra with curve fit for a full L3 cavity at 1386.1 nm and a decimated L3 cavity at 1387.4 nm.

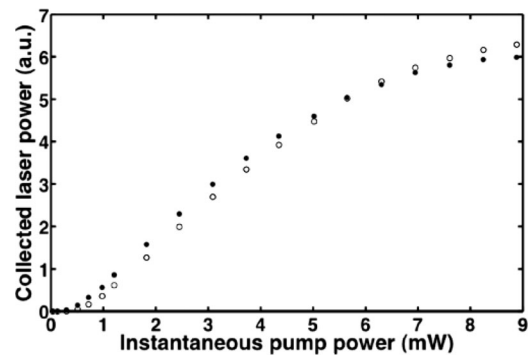


Fig. 6. Instantaneous light input versus collected light output for full L3 (filled circle) and decimated L3 (open circle) cavities.

lithography, and then used as a mask in an inductively coupled plasma reactive-ion etch process. Suspended membranes are then formed by removing the InP substrate underneath the photonic crystal areas using an HCl wet etch. Fig. 4(a) shows a SEM image of a decimated L3 cavity, and Fig. 4(b) shows a decimated H2 defect cavity. Note for both cavities, we have incorporated the same modifications of the holes nearest the cavity as for conventional L3 [4] and H2 designs [15]. The trenches around the photonic crystal assist in undercutting the cavity to create the suspended membrane. The lighter regions apparent in the images in Fig. 4 around the cavity denote the undercut area. For the decimated H2 cavity [see Fig. 4(b)], greater than half of the holes are omitted as compared to the complete H2 cavity laser.

IV. CHARACTERIZATION

The devices are tested at room temperature by optical pumping using a 980-nm laser diode. The excitation is 100-ns pulses with a 1% duty cycle. The pump light is focused onto the sample using a 20 \times objective, and the spot size is approximately 2–3 μ m. The laser emission is collected using the same objective and coupled to an optical spectrum analyzer that has a resolution of 0.06 nm. The device characteristics presented in Figs. 5 and 6 are for a decimated and complete L3 photonic crystal laser, with the dimensions described above. Fig. 5 shows the below threshold spectra for the L3 and decimated L3 cavities at 1386.1 nm

and 1387.4 nm, respectively. A fit to the data gives an upper limit to the quality factor for the full and decimated cavities to be 5022 and 4953, respectively. Random measurement error, spectrometer sensitivity, and slightly different pumping conditions among the cavities are likely causes of the difference in resonance wavelength and the quality factors being closer than the calculated values. Fig. 6 shows the instantaneous light input versus collected light output for both lasers. The characteristics for both devices are quite similar in optical performance. The linearly extrapolated lasing thresholds for the L3 and decimated L3 lasers are 0.37 and 0.46 mW, respectively. The approximately 20% threshold increase for the decimated L3 laser can be attributed to the difference in quality factor and pump variations previously mentioned.

In addition to the measurement of quality factor and threshold, a qualitative assessment of the thermal properties of the decimated L3 lasers is performed. Using the same optical pumping technique, the highest duty cycle operating conditions are determined. Adjusting both duty cycle and pulsewidth, the conditions for which the laser ceases stimulated emission are determined. In the case of the decimated L3 cavity, the device stops lasing when the duty cycle was set to 22% with a 300-ns pulse width. This is an improvement over the full L3 cavity, which requires a 100-ns pulse width and duty cycles less than 10%. This behavior is consistent with the decimated L3 cavity having decreased thermal impedance as compared to the full cavity.

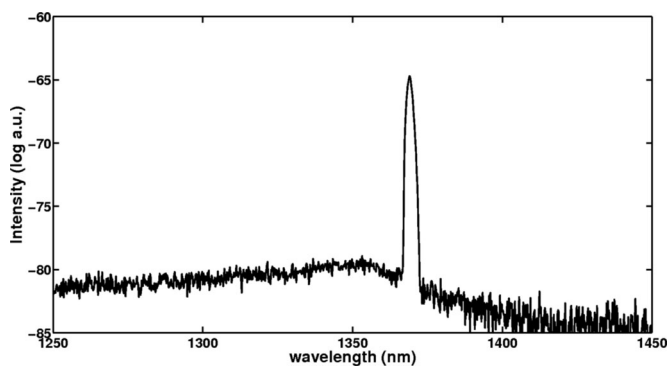


Fig. 7. Lasing spectrum of decimated H2 photonic crystal cavity.

The lasing spectrum of the decimated H2 cavity with $a = 470$ nm [see Fig. 4(b)] is shown in Fig. 7. Note that in this device, there are a minimum of two rows of holes surrounding the cavity. Thermal characteristics of this laser were probed as described previously. The device maintained laser operation up to a 27% duty cycle with 300-ns pulse width.

V. SUMMARY

In summary, we have demonstrated an approach that requires fewer holes around the defect cavity in photonic crystal defect membrane lasers. The decimated cavity designs are motivated by increasing of the fill factor of semiconductor material around the cavity to enhance electrical and thermal paths into the cavity. This approach is complementary to wafer bonding and may lead to further improvements in heat conduction if the two techniques are combined. Decimated lattice designs are developed using a field-intensity weighting algorithm that eliminates holes in circularly symmetric sectors around the defect cavity. Omission of photonic crystal holes in areas, where the field is minimal and where field symmetry negates coupling loss maintains the quality factor of the cavity. Both simulations and measurements of fabricated lasers indicate that there is no significant change in optical lasing characteristics between decimated and full lattice photonic crystal cavities. Qualitatively and quantitatively, the decimated L3 cavities also showed better thermal characteristics than the full lattice devices by maintaining operation at higher duty cycles and pulsewidth.

ACKNOWLEDGMENT

The authors would like to thank nLight Corp. and Dr. P. Leisher for the epitaxial material used in this paper.

REFERENCES

- [1] O. Painter, R. K. Lee, A. Scherer, A. Yariv, J. D. O'Brien, P. D. Dapkus, and I. Kim, "Two-dimensional photonic band-gap defect mode laser," *Science*, vol. 284, no. 5421, pp. 1819–1821, 1999.
- [2] H.-G. Park, J.-K. Hwang, J. Huh, H.-Y. Ryu, S.-H. Kim, J.-S. Kim, and Y.-H. Lee, "Characteristics of modified single-defect two-dimensional photonic crystal lasers," *IEEE J. Quantum Electron.*, vol. 38, no. 10, pp. 1353–1365, Oct. 2002.
- [3] Y. Akahane, T. Asano, B.-S. Song, and S. Noda, "High-Q photonic nanocavity in a two-dimensional photonic crystal," *Nature*, vol. 425, pp. 944–947, 2003.

- [4] Y. Akahane, T. Asano, B. Song, and S. Noda, "Fine-tuned high-Q photonic-crystal nanocavity," *Opt. Exp.*, vol. 13, no. 4, pp. 1202–1214, 2005.
- [5] K. Nozaki, T. Ide, J. Hashimoto, W.-H. Zheng, and T. Baba, "Photonic crystal point-shift nanolaser with ultimate small modal volume," *Electron. Lett.*, vol. 41, no. 15, pp. 843–845, 2005.
- [6] B. Ellis, T. Sarmiento, M. Mayer, B. Zhang, J. Harris, E. Haller, and J. Vuckovic, "Electrically pumped photonic crystal nanocavity light sources using a laterally doped p-i-n junction," *Appl. Phys. Lett.*, vol. 96, p. 181103, 2010.
- [7] T. Tanabe, K. Nishiguchi, E. Kuramochi, and M. Notomi, "Low power and fast electro-optic silicon modulator with lateral p-i-n embedded photonic crystal nanocavity," *Opt. Express*, vol. 17, no. 25, pp. 22505–22513, 2009.
- [8] H.-G. Park, S.-H. Kim, S.-H. Kwon, Y.-G. Ju, J.-K. Yang, J.-H. Baek, S.-B. Kim, and Y.-H. Lee, "Electrically driven single-cell photonic crystal laser," *Science*, vol. 305, no. 5689, pp. 1444–1447, 2004.
- [9] H.-G. Park, S.-H. Kim, M.-K. Seo, Y.-G. Ju, S.-B. Kim, and Y.-H. Lee, "Characteristics of electrically driven two-dimensional photonic crystal lasers," *IEEE J. Quantum Electron.*, vol. 41, no. 9, pp. 1131–1141, Sep. 2005.
- [10] C. M. Long, A. V. Giannopoulos, and K. D. Choquette, "Modified spontaneous emission from laterally injected photonic crystal emitter," *Electron. Lett.*, vol. 45, no. 4, pp. 227–228, 2009.
- [11] J. R. Cao, W. Kuang, Z.-J. Wei, S.-J. Choi, H. Yu, M. Bagheri, J. D. O'Brien, and P. D. Dapkus, "Sapphire-bonded photonic crystal microcavity lasers and their far-field radiation patterns," *IEEE Photon. Tech. Lett.*, vol. 17, no. 1, pp. 4–6, 2005.
- [12] G. Vecchi, F. Raineri, I. Sagnes, A. M. Yacomotti, P. Monnier, R. Braive, S. Bouhoule, A. Levenson, and R. Raj, "Continuous-wave operation of photonic band-edge laser at 1.55 μm on silicon wafer," *Proc. SPIE*, vol. 6593, pp. 7551–7556, 2007.
- [13] M. H. Shih, Y.-C. Yang, Y.-C. Liu, Z.-C. Chang, K.-S. Hsu, and M. C. Wu, "Room temperature continuous wave operation and characterization of photonic crystal nanolaser on a sapphire substrate," *J. Phys. D: Appl. Phys.*, vol. 42, 105113, 2009.
- [14] S.-K. Kim, G.-H. Kim, S.-H. Kim, Y.-H. Lee, S.-B. Kim, and I. Kim, "Loss management using parity-selective barriers for single-mode, single-cell photonic crystal resonators," *Appl. Phys. Lett.* vol. 88, 161119, 2006.
- [15] H.-Y. Ryu, M. Notomi, G.-H. Kim, and Y.-H. Lee, "High quality-factor whispering-gallery mode in the photonic crystal hexagonal disk cavity," *Opt. Express*, vol. 12, no. 8, pp. 1708–1719, 2004.
- [16] S. Matsuo, A. Shinya, T. Kakitsuka, K. Nozaki, T. Segawa, T. Sato, Y. Kawaguchi, and M. Notomi, "High-speed ultracompact buried heterostructure photonic-crystal laser with 13 fJ of energy consumed per bit transmitted," *Nat. Photon.*, vol. 4, pp. 648–654, 2010.



Antonios V. Giannopoulos (S'06) received the B.S. degrees in mathematics and electrical engineering and the M.S. and Ph.D. degrees in electrical and computer engineering from the University of Illinois, Urbana, in 2003, 2006, and 2010, respectively.

In 2010, he joined MicroLink Devices, Niles, IL, as a Research and Development Engineer, where he was engaged in research on multijunction solar cells. His current research interests include semiconductor device physics, design, and fabrication and novel semiconductor optical devices.



Joshua D. Sulkin (S'02) received the B.S. degree in computer engineering and the M.S. degree in electrical engineering from the University of Illinois, Urbana, in 2006 and 2007, respectively, where he is currently working toward the Ph.D. degree in the Photonic Device Research Group.

His research interests include photonic devices such as vertical-cavity surface-emitting lasers and photonic crystal membrane lasers.



Christopher M. Long (S'07) received the B.S. degrees in electrical engineering and physics from Kansas State University, Manhattan, in 2002, and the M.Sc. and Ph.D. degrees in electrical engineering from the University of Illinois, Urbana, in 2005 and 2008, respectively.

He is currently a Postdoctoral Researcher in ultrafast optics at Purdue University, West Lafayette, IN. His research interests include fabrication and characterization of photonic devices, and applications of optical pulse shaping in microwave photonics.



James J. Coleman (S'73–M'76–SM'80–F'92) received the B.S., M.S., and Ph.D. degrees in electrical engineering from the University of Illinois, Urbana.

He was with Bell Laboratories, Murray Hill, NJ, where he contributed to the development of long wavelength 1.3- μm InGaAsP CW room-temperature diode lasers grown by liquid phase epitaxy. He was also with Rockwell International, Anaheim, CA, where he studied metal-organic chemical vapor deposition grown low-threshold single-mode AlGaAs-GaAs double heterostructure and quantum-well heterostructure laser devices. He presently holds the Intel Alumni Endowed Chair in Electrical and Computer Engineering at the University of Illinois, Urbana.

He and his students were the first group to define experimentally the ranges of wavelength, threshold current density, and reliability of 980-nm strained-layer InGaAs lasers and they are presently involved in developing high-performance narrow-linewidth DBR lasers, integrable lasers and other photonic devices by selective-area epitaxy, and the growth processes for quantum-dot and quantum-wire lasers. He is the author or coauthor of more than 400 papers in technical journals and 13 book chapters. He has 7 U.S. patents and has given more than 90 invited presentations.

Prof. Coleman was an Associate Editor of IEEE PHOTONICS TECHNOLOGY LETTERS and as Guest Editor for two Special Issues of the IEEE JOURNAL OF QUANTUM ELECTRONICS and three other Special Issues of the IEEE JOURNAL OF SELECTED TOPICS IN QUANTUM ELECTRONICS. He is former chair of the IEEE Photonics Society (formerly LEOS) Semiconductor Lasers Technical Committee and was the Photonics Society Vice-President for publications. He is currently the President of the Photonics Society. He has won the IEEE David Sarnoff Award, the IEEE Photonics Society Distinguished Service Award, the OSA Nick Holonyak, Jr. Award, the ISCS Heinrich Welker Award, the IEEE Photonics Society William Streifer Scientific Achievement Award, and was an IEEE Photonics Society Distinguished Lecturer. He is a Fellow the Optical Society of America, the American Physical Society, and the American Association for the Advancement of Science.



Kent D. Choquette (M'97–F'03) received the B.S. degrees in engineering physics and applied mathematics from the University of Colorado, Boulder, and the M.S. and Ph.D. degrees in materials science from the University of Wisconsin, Madison.

He was a Postdoctoral Fellow at AT&T Bell Laboratories, Murray Hill, NJ. He then joined Sandia National Laboratories, Albuquerque, NM. Since 2000, he has been with the Electrical and Computer Engineering Department, University of Illinois, Urbana, where his Photonic Device Research Group is centered around the design, fabrication, characterization, and applications of vertical cavity surface-emitting lasers, photonic crystal light sources, nanofabrication technologies, and hybrid integration techniques for photonic devices. He has authored more than 200 technical publications and 3 book chapters, and has presented numerous invited talks and tutorials.

Dr. Choquette was an Associate Editor of the IEEE JOURNAL OF QUANTUM ELECTRONICS, IEEE PHOTONIC TECHNOLOGY LETTERS, and JOURNAL OF LIGHTWAVE TECHNOLOGY, as well as a Guest Editor of IEEE JOURNAL OF SELECTED TOPICS IN QUANTUM ELECTRONICS. He was awarded the 2008 IEEE/LEOS Engineering Achievement Award. He is a Fellow of the Optical Society of America and the International Society for Optical Engineers (SPIE).

Dr. Choquette was an Associate Editor of the IEEE JOURNAL OF QUANTUM ELECTRONICS, IEEE PHOTONIC TECHNOLOGY LETTERS, and JOURNAL OF LIGHTWAVE TECHNOLOGY, as well as a Guest Editor of IEEE JOURNAL OF SELECTED TOPICS IN QUANTUM ELECTRONICS. He was awarded the 2008 IEEE/LEOS Engineering Achievement Award. He is a Fellow of the Optical Society of America and the International Society for Optical Engineers (SPIE).